Oxidative stress-responsive microRNA-320 regulates glycolysis in diverse biological systems

Huibin Tang,[*,‖] Myung Lee,[*,‖] Orr Sharpe,[†,‡,‖] Louis Salamone,[†] Emily J. Noonan,[§,‖] Chuong D. Hoang,[*,‖] Sanford Levine,[¶] William H. Robinson,[†,‡,‖] and Joseph B. Shrager[*,‖,1]

[*]Division of Thoracic Surgery, Department of Cardiothoracic Surgery, [†]Department of Surgery, and [‡]Division of Immunology and Rheumatology and [§]Division of Hematology; Department of Medicine, Stanford University School of Medicine, Stanford, California, USA; [‖]Veterans Affairs Palo Alto Healthcare System, Palo Alto, California, USA; and [¶]Department of Surgery, University of Pennsylvania School of Medicine, Philadelphia, Pennsylvania, USA

ABSTRACT **Glycolysis is the initial step of glucose catabolism and is up-regulated in cancer cells (the Warburg Effect). Such shifts toward a glycolytic phenotype have not been explored widely in other biological systems, and the molecular mechanisms underlying the shifts remain unknown. With proteomics, we observed increased glycolysis in disused human diaphragm muscle. In disused muscle, lung cancer, and H_2O_2-treated myotubes, we show up-regulation of the rate-limiting glycolytic enzyme muscle-type phosphofructokinase (PFKm, >2 fold, $P<0.05$) and accumulation of lactate (>150%, $P<0.05$). Using microRNA profiling, we identify miR-320a as a regulator of PFKm expression. Reduced miR-320a levels (to ~50% of control, $P<0.05$) are associated with the increased PFKm in each of these diverse systems. Manipulation of miR-320a levels both *in vitro* and *in vivo* alters PFKm and lactate levels in the expected directions. Further, miR-320a appears to regulate oxidative stress-induced PFKm expression, and reduced miR-320a allows greater induction of glycolysis in response to H_2O_2 treatment. We show that this microRNA-mediated regulation occurs through PFKm's 3′ untranslated region and that Ets proteins are involved in the regulation of PFKm *via* miR-320a. These findings suggest that oxidative stress-responsive microRNA-320a may regulate glycolysis broadly within nature.—Tang, H., Lee, M., Sharpe, O., Salamone, L., Noonan, E. J., Hoang, C. D., Levine, S., Robinson, W. H., Shrager, J. B. Oxidative stress-responsive microRNA-320 regulates glycolysis in diverse biological systems. *FASEB J.* 26, 4710–4721 (2012). www.fasebj.org**

Key Words: phosphofructokinase · muscle · diaphragm · mechanical ventilation · Warburg effect · Ets

Cells use glucose to generate the energy [adenosine triphosphate (ATP)] that fuels all cellular processes. Glycolysis is the initial step in glucose catabolism, and its end products, in most tissues under most circumstances, are fed into mitochondrial oxidative phosphorylation. Since 30 of 36 ATP molecules generated during glucose breakdown derive from the Krebs cycle, mitochondria are generally the major source of cellular energy. Although glycolysis represents a less efficient form of ATP production than oxidative phosphorylation, it does play an important role in the bioenergetics of skeletal muscle (1). Glycolytic activity is up-regulated in skeletal muscles during increased physical activity, particularly under anaerobic conditions (2–4). Up-regulation of glycolysis also occurs in many pathological situations outside of skeletal muscle, such as in cancer progression (5, 6) and cellular proliferation (7).

Mitochondrial oxidative stress may be a primary cause of disordered cellular energy production in some of these scenarios. For example, cancer cells use primarily glycolysis to produce ATP, despite the presence of abundant oxygen, the so-called Warburg effect (or aerobic glycolysis; refs. 8, 9). This phenotype in cancer cells may stem from a mitochondrial defect (10–15) and/or from the particular requirement for a high-level building blocks for synthesis of proteins, nucleic acids, and lipids from the glycolytic intermediates during cancer cell proliferation (8, 16). Although the

Abbreviations: 2D-DIGE, 2-dimensional difference in-gel electrophoresis; ATP, adenosine triphosphate; EMSA, electrophoretic mobility shift assay; Ets-1, v-ets erythroblastosis virus E26 oncogene homolog 1; IEF, isoelectric focusing; IPG, immobilized pH gradient; LDH, lactate dehydrogenase; MALDI-TOF, matrix-assisted laser desorption ionization-time of flight; miR, microRNA; MS, mass spectrometry; MV, mechanical ventilation; NCBInr, National Center for Biotechnology Information nonredundant; PFKm, muscle-type phosphofructokinase; TA, tibialis anterior; UTR, untranslated region; VIDD, ventilation-induced diaphragm dysfunction

[1] Correspondence: Stanford University School of Medicine, 2nd floor, Falk Building, 300 Pasteur Dr., Stanford, CA 94305-5407, USA. E-mail: shrager@stanford.edu

doi: 10.1096/fj.11-197467

This article includes supplemental data. Please visit *http://www.fasebj.org* to obtain this information.

0892-6638/12/0026-4710 © FASEB

rom www.fasebj.org by Stanford University Libraries (171.65.8.159) on March 14, 2019. The FASEB Journal Vol. ${article.issue.getVolume()}, No. ${article.issue.getIssueNumber()},

underlying causes of the malignant glycolytic phenotype remain controversial, recent studies have shown that oxidative stress does directly contribute to tumor progression (17, 18). Further, alleviation of mitochondrial oxidative stress *via* transgenic overexpression of mitochondria-localized catalase is able to reduce tumor grade and metastasis (19). Thus, understanding whether and how oxidative stress is involved in this glycolytic phenotype may result in novel leads in cancer therapy.

We and others have also identified mitochondrial dysfunction in diaphragm muscle that is noncontracting as a result of full mechanical ventilatory support (20, 21). Although mechanical ventilation (MV) can be a life-saving intervention in patients with respiratory failure, prolonged MV is associated with the development of diaphragm dysfunction, which is a likely contributor to difficulty separating patients from the ventilator and subsequent complications. Both atrophy of diaphragmatic myofibers and reduced diaphragmatic contractility (*i.e.*, reduced specific force) are thought to contribute to ventilator-induced diaphragm dysfunction (VIDD; ref. 22). However, the pathogenesis of the "nonatrophy" component of VIDD remains relatively undeveloped. In a rodent MV model, it has been observed that the activities of key respiratory chain enzymes are reduced in MV diaphragm (20), and in human diaphragm, MV down-regulates genes involved in the mitochondrial respiratory chain (21, 22).

We hypothesized that this compromised mitochondrial function and the resulting oxidative stress in the diaphragm during MV might lead to increased glycolysis within diaphragmatic myofibers (similar to a proposed pathogenesis of the Warburg effect in cancers) and that this dependence on glycolysis and the consequently insufficient energy supply might provide an explanation for the reduced specific force of diaphragmatic contraction in these circumstances.

We first used proteomics to systemically profile the altered protein expression in MV human diaphragm, and this confirmed that there are important changes in glycolytic pathways. We then used microRNA microarray to examine the regulatory factors that control expression of the gene coding for the rate-limiting glycolytic enzyme phosphofructokinase (PFKm). Given the apparently similar pathogenetic bases of the increased glycolysis seen in MV diaphragm and in cancer cells, we then set out to determine whether the molecular mechanisms underlying this up-regulation are shared. We find that down-regulated microRNA (miR)-320a contributes to the up-regulated PFKm in disused diaphragm, in lung cancer, and in cultured muscle cells in response to oxidative stress. This novel, shared mechanism for increased glycolysis in response to mitochondrial dysfunction in both VIDD and cancer suggests a regulatory mechanism that may control glycolysis broadly across biological systems, as well as providing a potential therapeutic target for cancer.

MATERIALS AND METHODS

Human subjects

Our protocol for MV diaphragm biopsy subjects (organ donors ventilated at least 18 h before biopsy) was approved by the Gift of Life Donor Program, and our protocol for control subjects (typical patients undergoing thoracotomy ventilated 1–2 h prior to biopsy) was approved by the University of Pennsylvania and Stanford Institutional Review Boards. All biopsies were obtained with written informed consent. The inclusion criteria and collection details for MV human diaphragm, vastus, and their control muscles are described in detail in a previous report (21, 22). The human lung adenocarcinoma tissues and their normal control tissues were harvested during surgery at the Stanford and Veterans Affairs Palo Alto hospitals.

2-Dimensional difference in-gel electrophoresis (2D-DIGE) and protein identification with mass spectrometry (MS)

2D-DIGE and protein ID was performed in collaboration with Applied Biomics (Hayward, CA, USA) and the Veterans Affairs Palo Alto Mass Spectrometry Laboratory. Tissues were sonicated in lysis buffer [30 mM Tris-HCl, pH 8.8, containing 7 M urea, 2 M thiourea, and 4% 3-((3-cholamidopropyl) dimethylammonio)-propanesulfonate (CHAPS)]; the lysates were then centrifuged for 30 min at 14,000 rpm, and the supernatant was collected. Total 30-μg protein samples from control and MV groups were labeled with Cy2 and Cy5, respectively, and mixed together to run on immobilized pH gradient (IPG) stripes following the isoelectric focusing (IEF) protocol (Amersham BioSciences, Piscataway, NJ, USA). After the first-dimensional separation on IEF, the IPG strips were transferred into 13.5% SDS-gels. The SDS gels were run at 15°C until the dye front ran out of the gels. Gel images were scanned immediately following the SDS-PAGE using Typhoon TRIO (Amersham BioSciences). The scanned images were then analyzed by Image Quant 6.0 software (Amersham BioSciences), followed by in-gel analysis using DeCyder 6.0 software (Amersham BioSciences). The fold change of the protein expression levels was obtained from in-gel DeCyder analysis. The spots of interest were picked up by Ettan Spot Picker (Amersham BioSciences) based on the in-gel analysis and spot picking design by DeCyder software. The gel spots were digested in-gel with modified porcine trypsin protease (Trypsin Gold; Promega, Madison, WI, USA), desalted by Zip-tip C18 (Millipore, Beford, MA, USA), and subjected to MS for protein identification.

Matrix-assisted laser desorption ionization-time of flight (MALDI-TOF) MS and TOF/TOF tandem MS were performed on an ABI 4700 mass spectrometer (Applied Biosystems, Foster City, CA, USA). MALDI-TOF mass spectra were acquired in reflection positive-ion mode, averaging 2000–4000 laser shots/spectrum. TOF/TOF tandem MS fragmentation spectra were acquired for each sample, averaging 2000–4000 laser shots/fragmentation spectrum on each of the 5–10 most abundant ions present in each sample to exclude trypsin autolytic peptides and other known background ions.

Both of the resulting peptide mass and the associated fragmentation spectra were submitted to GPS Explorer workstation equipped with MASCOT search engine (Matrix Science, Boston, MA, USA) to search the National Center for Biotechnology Information nonredundant (NCBInr) database (NCBI, Bethesda, MD, USA). Searches were performed without constraining protein molecular weight or isoelectric point, with variable carbamidomethylation of cysteine and oxidation of methionine residues, and with 1 missed cleavage also allowed in the search parameters. Candidates with either

om www.fasebj.org by Stanford University Libraries (171.65.8.159) on March 14, 2019. The FASEB Journal Vol. ${article.issue.getVolume()}, No. ${article.issue.getIssueNumber()},

protein score confidence interval percentage (CI%) or Ion CI% > 95 were considered significant.

cDNA cloning and plasmid construction

Total RNAs were reverse transcribed with Superscript II, and cDNA was amplified with PCR by Hi-Fi *Taq* polymerase. Amplified v-ets erythroblastosis virus E26 oncogene homolog 1 (Ets-1) cDNA was cloned into pcDNA3.1/NT-GFP-TOPO vector. The 3′-untranslated region (UTR) cDNA fragments of PFKm were cloned into pMIR-REPORT luciferase between *Spe*I and PmeI. The 5′ DNA flanking sequence (promoter) of miR-320a (~1 kb) was cloned into a pEL-luciferase vector between *Hind*III and *Bam*HI. The point mutations were performed with QuickChange site-directed mutagenesis kit (Agilent/Stratagene, Santa Clara, CA, USA). Primers used for PCR were Ets-1 cDNA: forward, GCCCCCTCAACTCCGGGCACC, reverse, CATGACTAGTCAGCATCCGG; and 3′-UTR of PFKm: forward, GATCGACTAGTACCTCTCTGGAGTGAGGGGAATA, reverse: GGATAGTTTAAACCACAGTGACCAGTTGGCATTT. Promoter of miR-320 was forward, TGATCAAGCTTCCACAGAGTTATGAACACTCG, reverse, AATCAGGATCCGAGGCCGTCGGATAAATAC. Primers for the PFKm 3′-UTR mutations were mut1 (mutated nucleotides underscored): CATGACTTCTGCCCTATCATGATCTGTCACACAAG; and mut2: TTCCTAAAAATAATCACTGTTTATTTCTTTGTGAT. Primer for Ets binding site mutation in miR-320a promoter was GAGCCCAGAACATAATAAGCACGTCTGGCTGTCTTGAATCAACTAGATTCACTGTC.

Cell culture, gene transfection, stable line, and reporter gene assay

C2C12 cells were cultured in 10% fetal bovine serum (FBS) and Dulbecco's modified Eagle's medium (DMEM). Anti-microRNAs and pre-microRNAs were all purchased from Ambion. They were transfected into C2C12 cells with Lipofectamine 2000 (Invitrogen, Carlsbad, CA, USA) at a final concentration of 40 μM. After 3 d, proteins were collected from the transfected cell for assays. Constitutive Ets-1 expressed C2C12 cell line was selected after transfection with Ets-1 expression vector with G418 (400 μg/ml) for 2 wk, and the pooled selected cells were used for the experiment, with parental c2c12 cells as control.

Gene electroporation was performed as described previously (23). Briefly, 320 nmol pre-miR-320a or pre-miR-control (Ambion, Austin, TX, USA) was mixed with 4 μg pCS2-GFP plasmid and electroporated into tibialis anterior (TA) muscle, respectively. After 7 d, the TA muscles were collected, and GFP^+ fibers were isolated under fluorescent dissection scope. Total protein was extracted from the GFP^+ fibers by RIPA buffer and then subjected to Western blot analysis.

The PFKm-3′UTR reporter genes pMIR-reporter-PFKm3′UTR (wild-type and their mutants), as well as the miR-320a promoter reporter gene, were transfected into C2C12 cells with Lipofectamine 2000, together with pre-miR-320a, anti-miR-320a, or pcNDA3.1 Ets-1, as indicated. After 3 d, the cells were lysed and subjected to luciferase assay with Bright-Glo assay kit (Promega) on a luminometer (GloMax 20/20, Promega). The luciferase light values were normalized to β-Gal activity from the cotransfected control plasmid CS2-β-Gal.

Protein extraction and Western blotting

Total cellular proteins were extracted with modified lysis buffer [0.6 mM 4-(2-hydroxyethyl)-1-piperazineethanesulfonic acid (HEPES), 1 M $MgCl_2$, and 1.7 M KCl] with protease inhibitors (Complete Mini; Roche, Indianapolis, IN, USA). Proteins (5–15 μg) were separated by 4-12% SDS-PAGE gel for Western blot analysis. Primary antibodies (1:1000 in 5% milk in TBST) were anti-PFK-1 (muscle type, H-55; Santa Cruz Biotechnology, Santa Cruz, CA, USA) and anti-lactate dehydrogenase (LDH)a (Cell Signaling Technology, Danvers, MA, USA). The secondary antibody was horseradish peroxidase-conjugated anti-rabbit IgG. SuperSignal West Pico Chemiluminescent Substrate (ThermoScientific, Waltham, MA, USA) was used to detect the signals, and the resulting images were captured by the ChemiDoc XRS System (Bio-Rad, Hercules, CA, USA) for analysis.

Electrophoretic mobility shift assay (EMSA)

The protein and DNA binding ability was measured by EMSA. Briefly, oligo probe was synthesized by Invitrogen with biotin labeled at the 5′ end. Oligos of Ets-mutated probe and Ets consensus probe were used for binding competition. *In vitro* protein translation was performed by TnT Quick Coupled Transcription/Translation kit (Promega) with pcDNA3.1-Ets-1 plasmid as template. Nuclear extracts from C2C12 cells ($\pm H_2O_2$ for 4 h at 40 μM) were acquired through standard procedure. DNA:protein binding assay was performed and detected with LightShift Chemiluminescent EMSA kit (Thermo Scientific) by following the manufacturer's instructions. The sequence of the DNA probe was GCACTTCCGGATGT. The competition DNAs used were the known Ets-1 selected consensus sequence ACCGGAAGT (24) and the Ets site mutated DNA fragment (GAGCCCAGAACATAATAAGCACGTCTGGCTGTCTTGAATCAACTAGATTCACTGTC; mutated nucleotides underscored).

MicroRNA microarray and data analysis

MicroRNA microarray was performed at the Stanford microarray core facility. Briefly, total RNA was extracted from control (n=4) and MV (n=4) diaphragm with Trizol, and quality was analyzed with an Agilent Bioanalyzer. RNA (100 ng/sample) was used for single-color microarray on an Agilent microRNA microarray platform. MicroRNA data were further analyzed by GeneSpring GX11 (Agilent). The significantly altered entities were determined at a cutoff of $P < 0.05$ with multiple test correction.

Quantitative PCR for mRNA and microRNA

Total RNA was isolated with Trizol (Invitrogen). cDNA synthesis was done with SuperScript II RT kit (Invitrogen), and qPCR for mRNA quantification was performed with SYBR Green ROX Mix (ThermoScientific). Primers are pFKm forward, GGTCCGACACAGTCTCCTGGACCAG, reverse, CCCAGGGTTTTGGCTGCATGGT; and Ets-1 forward, CAGGATCTGCTCTCCGGCAAAGTA, reverse, CTTGCCTCACCACTGCAGGACG. Reverse transcription for microRNA quantification was performed using TaqMan MicroRNA RT Kit (Applied Biosystems) with 20 ng total RNA. qPCR was performed with TaqMan Small RNA Assay system (Applied Biosystems). U6b was used as an internal control.

Biochemical assays

The ATP (Biovision, Milpitas, CA, USA), lactate (Eton, Palo Alto, CA, USA), and pyruvate (Cayman, Ann Arbor, MI, USA) assays were performed per the manufacturers' instructions. Total protein (20 μg) from cell extracts was used in the assays. The absorbance level was measured at 490 nM using a

rom www.fasebj.org by Stanford University Libraries (171.65.8.159) on March 14, 2019. The FASEB Journal Vol. ${article.issue.getVolume()}, No. ${article.issue.getIssueNumber()},

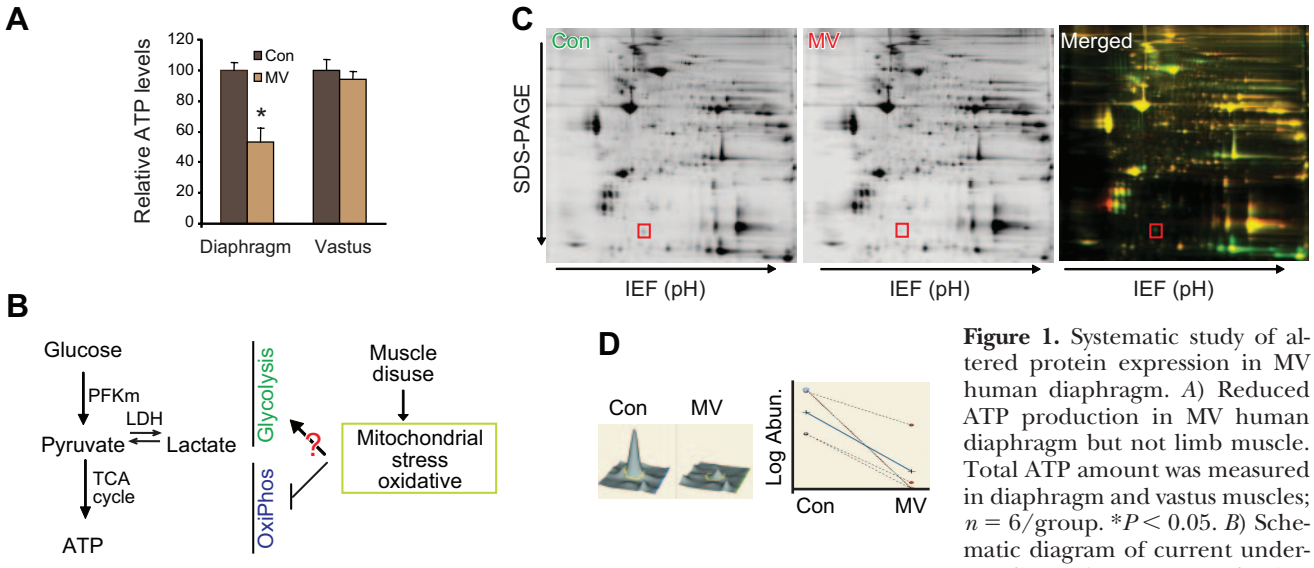

Figure 1. Systematic study of altered protein expression in MV human diaphragm. *A*) Reduced ATP production in MV human diaphragm but not limb muscle. Total ATP amount was measured in diaphragm and vastus muscles; $n = 6$/group. $^*P < 0.05$. *B*) Schematic diagram of current understanding of energy production within diaphragm myofibers subjected to MV. *C*) Representative 2-D DIGE gel proteomics. Control proteins are labeled green; MV proteins are labeled red. An example of a protein that is differentially identified in MV *vs.* control is highlighted by a red box. *D*) Analytic results of protein expression using Decyder software. A representative result is shown for the protein noted in the red box in *C*, and the right panel shows the variation among the 4 pairs of samples [MV *vs.* control (con)]. See Table 2 for summary of the results of proteomics. Significance level was set at $P < 0.05$. See Table 3 for results of DAVID bioinformatics and the altered KEGG pathways. Note that glycolytic pathways are by far the most common among the significantly altered pathways ($P<0.05$).

microplate reader. The concentrations of the metabolites were calculated using the standards included in the kit.

Bioinformatics and statistical analysis

Bioinformatics analysis was performed with the Database for Annotation, Visualization, and Integrated Discovery (DAVID; http://david.abcc.ncifcrf.gov/) and the KEGG pathway (http://www.genome.jp/kegg/pathway.html). Quantitative results are expressed as means ± SE. Student's *t* test was used to determine significance. Values of $P < 0.05$ was considered significant. The statistics in the microarray and 2D-DIGE experiments were calculated by Genespring GX and Decyder software, respectively, using $P < 0.05$ as cutoff for significance.

RESULTS

ATP level is low, and proteomics show that glycolysis is up-regulated, in human diaphragm muscle that is noncontractile as a result of MV

To explore the changes in energy metabolism within the diaphragm during disuse resulting from MV, we first measured total ATP level. Diaphragm disuse is associated with a dramatic reduction in measurable ATP. Notably, ATP levels are not significantly altered in the nonrespiratory vastus lateralis muscle (**Fig. 1*A***), indicating that altered skeletal muscle energy metabolism during MV is specific to ventilatory muscle. It has been reported that MV disables mitochondrial oxidative phosphorylation (20, 21), which would be expected to reduce ATP production. However, it has been unknown whether MV influences glycolysis (Fig. 1*B*). To systemically search for these changes, we employed proteomics with 2D-DIGE (Fig. 1*C*, *D* and **Table 1**). With 4 paired diaphragm samples, 102 protein spots were significantly changed at expression levels ($P<0.05$; Supplemental Fig. S1). These proteins that were differentially expressed between MV and control diaphragm were subjected to MS for protein identification. Forty-three unique proteins were up-regulated and 24 were down-regulated in MV diaphragm (Supplemental Tables S1 and S2). Using the DAVID bioinformatics tool to identify the altered pathways, we found that glycolysis was the most significantly influenced pathway (**Table 2**). Remarkably, proteins related to metabolic changes, such as glycolysis, pyruvate metabolism, and the citric acid cycle constituted 30% of the significantly altered proteins.

PFKm and glycolysis are increased in disused diaphragm muscle

Based on the 2D-DIGE results, 10 glycolytic enzymes are significantly induced in MV human diaphragm (**Table 3**),

TABLE 1. *Summary of the results of proteomics*

Category	Data
Samples	Human diaphragm muscle (MV *vs.* control)
Methods	2D-DIGE, MS
Results	
Unique proteins identified,	67
Proteins up-regulated	43
Proteins down-regulated	24
P	<0.05

om www.fasebj.org by Stanford University Libraries (171.65.8.159) on March 14, 2019. The FASEB Journal Vol. ${article.issue.getVolume()}, No. ${article.issue.getIssueNumber()},

TABLE 2. *Results of DAVID bioinformatics and the altered KEGG pathways*

KEGG pathway	Count	*P*
Glycolysis/gluconeogenesis	11	1.80E-12
Pyruvate metabolism	7	1.50E-07
Pentose phosphate pathway	4	5.20E-04
Galctose metabolism	4	5.80E-04
Fructose and mannose metabolism	4	1.30E-03
Tight junction	6	1.50E-03
Hypertrophophic cardiomyopathy	5	2.10E-03
Dilated cardiomyopathy	5	2.70E-03
Citrate cycle (TCA cycle)	3	1.70E-02
Starch and sucrose metabolism	3	3.00E-02
Regulation of actin cyctoskeleton	5	4.90E-02

including the rate-limiting enzyme of glycolysis, PFKm. Interestingly, dihydrolipoamide dehydrogenase, a component of pyruvate dyhydrogenase complex, is significantly reduced, implying that pyruvate-to-acetyl CoA conversion may be compromised. In conjunction with the elevated PFKm and LDH, this regulatory pattern might favor the conversion of pyruvate into lactate, rather than to acetyl CoA that feeds into Krebs cycle. Using Western blot analysis, we confirmed the elevated expression of PFKm and LDHa in MV human diaphragm at the protein level (**Fig. 2*A***). The mRNA level of PFKm is also modestly induced in MV diaphragm, although this is less impressive than the change seen at the protein level, suggesting that there might be post-transcriptional regulation of PFKm (Fig. 2*B*). In contrast, the levels of PFKm and LDHa in the nonrespiratory muscle, the vastus lateralis, do not change with MV (Fig. 2*C*). As a crude measure of enzymatic activity, we measured the metabolite of glucose metabolism, lactate, in MV human diaphragm and limb muscle. The lactic acid level is significantly elevated in MV diaphragm tissue *vs.* control (Fig. 2*D*), but not in vastus lateralis muscle, indicating that MV is associated with accumulation of lactate in respiratory muscle specifically during MV with diaphragm inactivity.

PFKm and glycolysis are also up-regulated in human lung adenocarcinoma and in an *in vitro* muscle cell oxidative stress model

It has been reported that glycolysis is increased in mouse lung tumors and human lung adenocarcinoma (consistent with the Warburg effect; refs. 25, 26), but the protein levels of the glycolytic enzymes, PFKm and LDHa, have not been reported in human lung adenocarcinoma. Using Western blot analysis, we find that PFKm and LDHa are each up-regulated in lung adenocarcinoma tissue *vs.* normal human lung tissue (**Fig. 3*A***). Consistently, the lactate level in adenocarcinoma is also increased (Fig. 3*B*).

We have demonstrated previously that mitochondrial oxidative stress is an upstream event inducing catabolic pathways that appear important in causing VIDD (21); mitochondrial defects and associated oxidative stress have also been demonstrated to occur in cancer cells (10–15, 17–19). We therefore hypothesized that mitochondrial oxidative stress may underlie the metabolic shift to a glycolytic phenotype in both of these systems. To explore whether oxidative stress is sufficient to induce these changes in energy metabolism, we examined the effect of H_2O_2-induced oxidative stress on glycolytic enzyme expression in cultured muscle cells. We find that PFKm is indeed up-regulated in this *in vitro* oxidative stress model (Fig. 3*C*). The level of ATP is reduced, and lactate is increased (Fig. 3*D*, *E*). These results are strikingly similar to the observations in MV human diaphragm and human lung cancer tissue detailed above. It thus appears that oxidative stress may be a central mechanism in the up-regulation of glycolysis seen in cancer and disused diaphragm.

MicroRNA-320a regulates the expression of PFKm

Because the up-regulation of PFkm, the key regulator of glycolytic efficiency, is robust at the protein level but relatively modest at the mRNA level (Table 3 and Fig. 2), we suspected that regulation might occur post-transcriptionally, *e.g.*, *via* microRNAs. To test this hypothesis, we searched for possible microRNA regulators by carrying out microRNA microarray on MV human diaphragm samples. The results demonstrate that 278 microRNAs are significantly ($P<0.05$) down-regulated (by 1.7- to 6-fold), while 3 are up-regulated (by 2- to 6-fold; **Fig. 4*A*** and Supplemental Table S3). To determine whether any of these altered microRNAs are potential regulators of PFKm, we first used TargetScan to search for the microRNA candidates. Comparing these predicted microRNA candidates with the altered microRNAs in our microarray, we identified miR-320a as 1 potential microRNA involved in the regulation of PFKm in disused diaphragm (Fig. 4*B*). MiR-320a is a member in the broadly conserved miR-320 family in vertebrates that targets conserved sites on the PFKm 3′ UTR, and miR-320a is significantly down-regulated by MV in our microRNA microarray.

To validate the role of miR-320a in regulating PFKm and thereby glycolysis, we first validated the

TABLE 3. *Altered glycolytic enzymes identified by MS*

Altered protein in glycolysis pathway	Fold change (MV/control)
Aldolase A, fructose-bisphosphate	2.1 ×
Aldolase C, fructose-bisphosphate	1.5 ×
Dihydrolipoamide dehydrogenase	−2.1 ×
Glyceraldehyde-3-p-dehydrogenase	1.5 ×
Lactate dehydrogenase A	2.1 ×
Lactate dehydrogenase B	1.7 ×
Phosphofructokinase, muscle	2.3 ×
Phosphoglucomutase 1	2.4 ×
Phosphoglycerate kinase 1	1.5 ×
Pyruvate dehydrogenase α 1	1.6 ×
Pyruvate kinase, muscle	2.0 ×

Cutoff was set at fold change > 1.5; $P < 0.05$.

rom www.fasebj.org by Stanford University Libraries (171.65.8.159) on March 14, 2019. The FASEB Journal Vol. ${article.issue.getVolume()}, No. ${article.issue.getIssueNumber()},

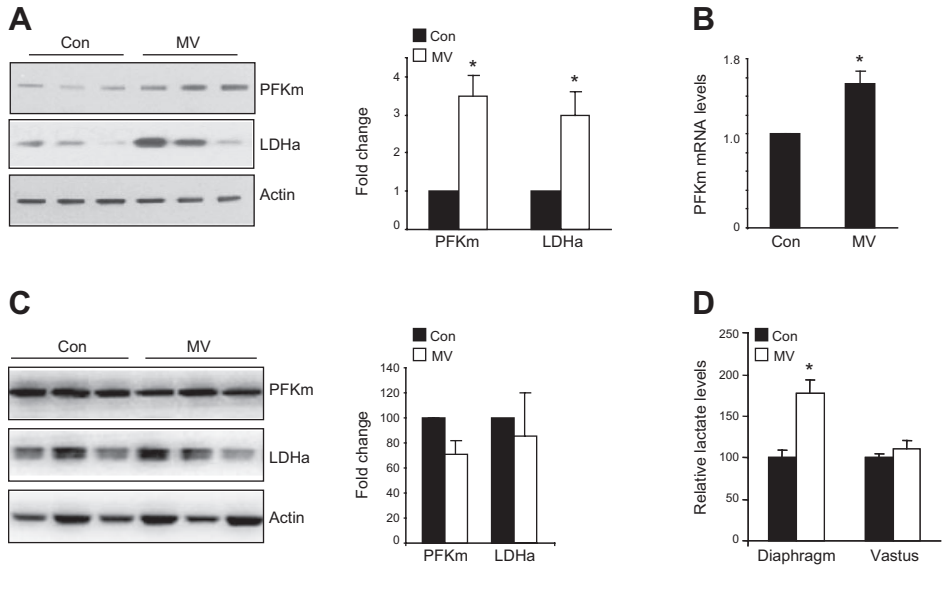

Figure 2. MV up-regulates glycolytic enzymes in human diaphragm muscle. See Table 3 for list of altered glycolytic enzymes identified by MS. Cutoff was set at fold change > 1.5; $P < 0.05$. *A*) Representative Western blot analysis of PFKm and LDHa in human diaphragm. Fold change was calculated after normalizing the expression levels of PFK and LDHa to actin (for fold change, n=3/group. Con, control. *B*) mRNA expression of PFKm in diaphragm by real-time PCR (n=6/group). *C*) Representative Western blot of PFKm and LDHa in vastus lateralis muscle (a nonrespiratory, limb muscle). No significant difference was found between control and MV samples in this nonrespiratory muscle (n=3/group). *D*) Lactate levels in MV and control diaphragm and vastus muscle (n=6). *$P < 0.05$.

expression of miR-320a by real-time PCR in each of our experimental systems. MiR-320a is in fact down-regulated in MV human diaphragm *vs.* control, lung adenocarcinoma *vs.* normal lung tissue, and H_2O_2-treated C2C12 cells *vs.* untreated cells (Fig. 4*C*). To investigate whether miR-320a indeed regulates PFKm, we transfected microRNA mimics (pre-miR) and a microRNA antagonist (anti-miR) to manipulate the intracellular levels of microRNAs in cultured muscle cells. As shown in Fig. 4*D*, intracellular miR-320a is induced 250-fold (40 nM) and 300-fold (100 nM) following pre-miR transfection. On the contrary, anti-miR-320a results in ~95% reduction of endogenous miR-320a levels. Anti-miR-320a (40 nM) increased PFKm at the protein level, while overexpression of pre-miR-320a (40 nM) suppressed PFKm levels (Fig. 4*D*). We also tested the miR-320a effect in the A549 lung cancer cell line, and a similar regulatory effect was observed (Fig. 4*E*).

To establish that this microRNA-mediated regulation occurs specifically *via* the PFKm transcript, we constructed a reporter gene by linking the 3′ UTR of the PFKm transcript to a luciferase coding sequence (Fig. 4*F*). This reporter construct was cotransfected with miR-320a mimics and antagonists. The reporter activity was induced by anti-miR-320a and suppressed by pre-miR-320a (Fig. 4*F*), similar to the endogenous protein regulation. On the contrary, the reporter gene with mutations of both potential UTR sequences complementary to miR-320a was not influenced by cotransfected microRNAs (Fig. 4*F*). The same result was obtained using a reporter gene without the UTR sequence (Fig. 4*F*).

MiR-320a regulates glycolysis *in vitro* and *in vivo* and participates in oxidative stress-induced expression of PFKm

Beyond its impact on PFKm expression, knockdown of miR-320a in cultured C2C12 cells also results in increased lactate levels (**Fig. 5*A***). Interestingly, knockdown of miR-320a sensitizes the cells to H_2O_2-induced oxidative stress; *i.e.*, the induction of lactate in response to H_2O_2-induced oxidative stress is greater following knockdown of miR-320a (Fig. 5*B*). We further demonstrated that miR-320a mediates oxidative stress-induced PFKm expression and glycolysis. Pre-miRs of control or miR-320a were transfected into cultured C2C12 cells; 3 d later, cells were treated with 40 μM H_2O_2 for 24 h. H_2O_2-induced lactate level (Fig. 5*C*) and PFKm protein (Fig. 5*D*) were blocked in pre-miR-320a-transfected cells.

To evaluate whether miR-320a regulates glycolysis *in vivo*, we electroporated pre-miR-320a into mouse TA muscle. We find that the miR-320a level is induced up to 100-fold following electroporation of pre-miR-320a (Fig. 5*E*). With this increase in miR-320a concentration in skeletal muscle *in vivo*, there is a reduction in lactate level (Fig. 5*F*) and PFKm expression (Fig. 5*G*), as predicted by the *in vitro* experiments.

Expression of miR-320a is regulated by Ets-1 transcription factor

In an effort to understand how miR-320a is regulated in response to oxidative stress-associated events such as those known to be present in our human VIDD, human cancer, and *in vitro* H_2O_2-treated muscle cell models, we focused on Ets proteins. We chose Ets proteins because they are known to participate in the regulation of both cell progression and energy metabolism (27). We find that Ets-1 expression is in fact increased in MV human diaphragm, lung cancer, and C2C12 cells in response to H_2O_2 treatment, *vs.* each of their controls (**Fig. 6*A–C***).

To determine whether Ets proteins are able to regulate the expression of miR-320a, C2C12 cells were transfected with an Ets-1 constitutive expression vector. Overexpression of Ets-1 suppresses the expression of

om www.fasebj.org by Stanford University Libraries (171.65.8.159) on March 14, 2019. The FASEB Journal Vol. ${article.issue.getVolume()}, No. ${article.issue.getIssueNumber()},

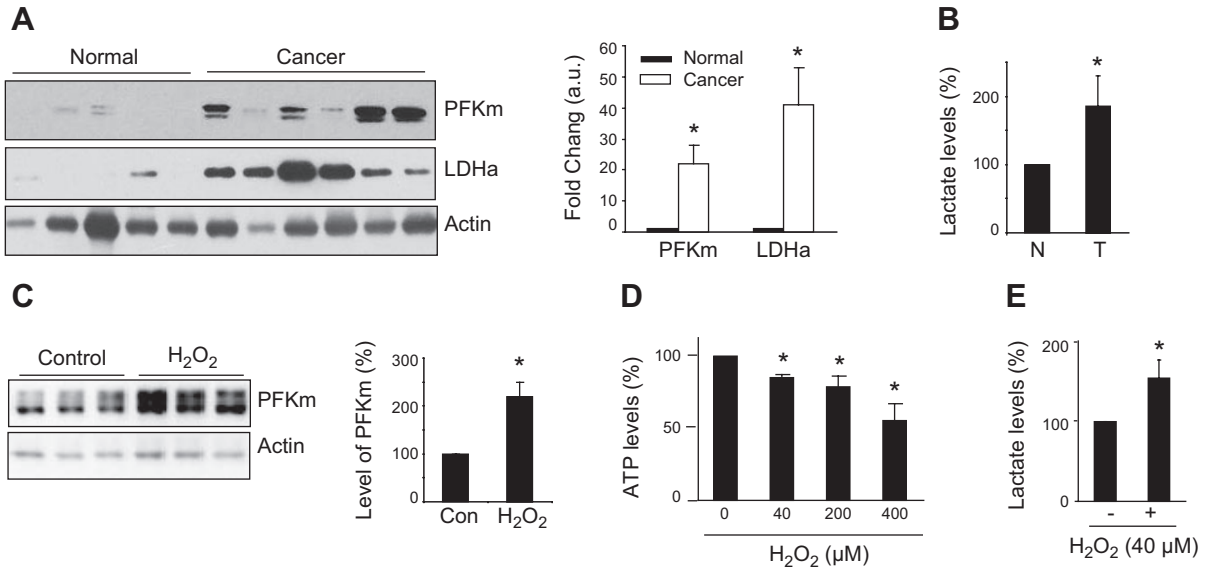

Figure 3. Increased glycolysis in human lung adenocarcinoma and muscle cells treated with H_2O_2. *A*) Protein expression of PFK and LDHa by Western blot in normal lung and lung adenocarcinoma. Fold change was calculated after normalizing to actin level (normal, $n=5$; cancer, $n=6$, $P<0.05$). *B*) Lactate level in lung adenocarcinoma (T) *vs.* normal lung (N) ($n=6$/group). *C*) Protein level of PFKm in cultured C2C12 muscle cells in response to H_2O_2 treatment (40 μM, 1h; $n=3$/group). Con, control. *D, E*) ATP (*D*) and lactate(*E*) (40 μM H_2O_2, 1 h) levels in cultured, H_2O_2-treated C2C12 muscle cells ($n=3$/dose level). $*P<0.05$.

miR-320a (Fig. 6*D*) and results in up-regulation of PFKm (Fig. 6*E*). Introduction of pre-miR-320a into Ets-1 overexpressing C2C12 cells blocks the Ets-1 induced PFKm expression (Fig. 6*F*), indicating that Ets-1 induced PFKm *via*, at least in part, reduction of miR-320a.

We next cloned the miR-320a promoter sequence and found that there is a conserved Ets binding site in the promoter sequence. The miR-320a promoter reporter construct was then cotransfected with the Ets-1 vector, and we found that promoter activity was significantly suppressed (Fig. 6*G*), whereas the promoter reporter with a mutated Ets binding site was not significantly influenced. We further examined by EMSA whether this predicted Ets binding DNA element can bind Ets protein. *In vitro* translated Ets protein was able to bind to this DNA element (Fig. 6*H*, left panel). The nuclear extract from C2C12 muscle cells can also bind to this DNA element, and the binding ability is induced by H_2O_2 treatment. However, Ets-1-selected consensus DNA sequence, but not the Ets-mutated sequence, strongly competed with this DNA:protein interaction (Fig. 6*H*, right panel). Taken together, these experiments demonstrate that the Ets-1 protein regulates miR-320a and contributes to the shift to a glycolytic phenotype.

DISCUSSION

We show here for the first time that glycolytic activity is increased in diaphragm tissue that is noncontractile as a result of full mechanical ventilatory support. We also confirm that the Warburg effect, *i.e.*, the up-regulation of glycolysis, is present in lung adenocarcinoma, and we show that the rate-limiting glycolytic enzyme PFKm is induced in disused diaphragm, lung cancer, and our *in vitro* model of oxidative stress (cultured myotubes treated with H_2O_2). Finally, we demonstrate that the up-regulation of glycolysis in these widely divergent biological systems share a regulatory apparatus composed of microRNA-320a and Ets-1 (**Fig. 7**).

The prolonged use of MV has been demonstrated in both human (22, 28, 29) and animal models (30, 31) to result in diaphragm weakness (VIDD). This weakness is one likely cause of ventilator weaning difficulties that may result in a cascade of additional complications that dramatically increase morbidity, mortality, and costs in intensive care unit patients. The pathogenesis of VIDD appears to include 2 components: diaphragm myofiber atrophy resulting from activation of catabolic cascades; and reduced contractility of myofibers unrelated to atrophy (*i.e.*, reduced specific force). A great deal of attention has been focused on the mechanisms underlying the atrophy component of VIDD (28, 30), including from our group, while far less attention has been directed to the reduced contractility component.

The identification here of increased glycolysis and lactate accumulation in MV diaphragm represents a potential pathogenetic mechanism for this second, "dysfunction" component of VIDD. Our demonstration of reduced total ATP levels in MV human diaphragm suggests that the demonstrated shift to glycolysis, with its less efficient production of ATP, leaves the diaphragm with a relative lack of energy for contraction. Further, although controversial (32), intramuscular lactate accumulation itself may contribute to muscle

rom www.fasebj.org by Stanford University Libraries (171.65.8.159) on March 14, 2019. The FASEB Journal Vol. ${article.issue.getVolume()}, No. ${article.issue.getIssueNumber()},

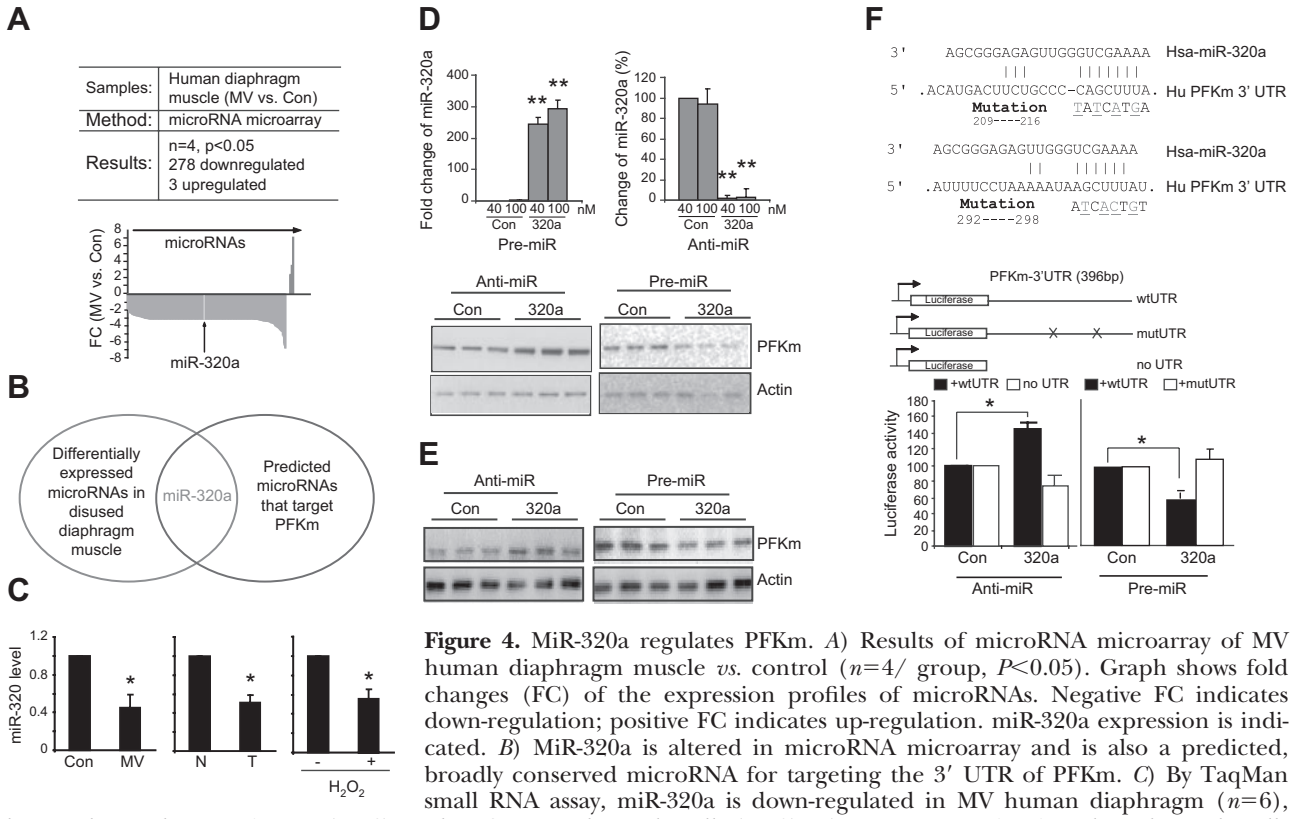

Figure 4. MiR-320a regulates PFKm. *A*) Results of microRNA microarray of MV human diaphragm muscle *vs.* control (n=4/ group, P<0.05). Graph shows fold changes (FC) of the expression profiles of microRNAs. Negative FC indicates down-regulation; positive FC indicates up-regulation. miR-320a expression is indicated. *B*) MiR-320a is altered in microRNA microarray and is also a predicted, broadly conserved microRNA for targeting the 3′ UTR of PFKm. *C*) By TaqMan small RNA assay, miR-320a is down-regulated in MV human diaphragm (n=6), human lung adenocarcinoma (n=6), and H_2O_2-treated muscle cells (n=3). *D*) PFKm expression in cultured muscle cells is regulated by miR-320a. Anti- and pre-miR-320a, respectively, was transfected into C2C12 cells for 3 d. qPCR was performed to measure the levels of intracellular miR-320a, and Western blot was performed to detect PFKm protein. *E*) PFKm expression in cultured A549 lung cancer cells is regulated by miR-320a. Anti- and pre-miR-320a, respectively, was transfected into A549 cells for 3 d, and Western blot was performed to detected PFKm protein. *F*) MiR-320a regulates PFKm through the 3′ UTR of PFKm. Reporter gene was constructed by inserting the wild-type or the mutated 3′-UTR sequence of the PFKm transcript into the 3′ end of the luciferase gene. Mutated sequences are underscored. Reporter gene assay was performed to detect the effect of miR-320a after cotransfection with either anti- or pre-miR-320a (n=3). Luciferase value was normalized to β-Gal activity from the cotransfected plasmid CS2-β-Gal. *$P < 0.05$, **$P < 0.01$.

fatigue and dysfunction. In skeletal muscle *in vivo*, lactate down-regulates the glycolytic enzymes hexokinase (HK) and PFKm (33). Thus, lactate accumulation may limit the amount of energy that can be produced by glycolysis in compensation for reduced oxidative phosphorylation. Lactate accumulation also inhibits lipolysis, reducing another potential source of energy for diaphragm contraction (34).

The up-regulation of glycolysis in malignant tumors has been termed the Warburg effect. Interestingly, the glycolytic phenotype in MV human diaphragm appears to closely mimic the Warburg effect seen in lung adenocarcinoma. Although glycolysis produces less ATP per glucose molecule than mitochondrial oxidative phosphorylation, glycolysis can provide energy rapidly since it operates at a rate 100 times faster than that of oxidative phosphorylation. In cancer cells, this facilitated glycolysis has been linked to the supply of both energy and of the building blocks for the synthesis of proteins, nucleic acids, and lipids, which are needed for cell proliferation, as well as to lactate-induced microenvironmental acidosis which drives the selection of acid-resistant cancer cells that are thought to contribute to proliferation and invasion (35).

In disused diaphragm, this shift to a glycolytic phenotype may represent a cellular protective mechanism activated to compensate for the reduced energy supply resulting from compromised mitochondria. It remains to be explored whether the increased glycolytic metabolites in disused diaphragm muscle may also supply building blocks for the proliferation of cells near muscle fibers, since it has been reported that limb muscle disuse causes the proliferation of interstitial cells, such as fibroblasts, capillary endothelial cells, and inflammatory cells (36).

Although we and others (37, 38) have shown that oxidative stress (H_2O_2 treatment) is able to induce glycolysis in cultured cells, it has also been reported that, in contrast, oxidative stress suppresses glycolysis in some *in vitro* culture models. For example, H_2O_2-induced oxidative stress inhibits glycolysis in astrocyte and U937 cells (39, 40). The consequences of cellular oxidative stress appear to depend on the sensitivity of the cells studied to H_2O_2, as well as the intensity and duration of the H_2O_2 treatment. The available data suggest that elevation of glycolysis is a cellular adaptive response to milder oxidative stress (sublethal dose of H_2O_2,) experienced for a briefer period, under which

rom www.fasebj.org by Stanford University Libraries (171.65.8.159) on March 14, 2019. The FASEB Journal Vol. ${article.issue.getVolume()}, No. ${article.issue.getIssueNumber()}, p

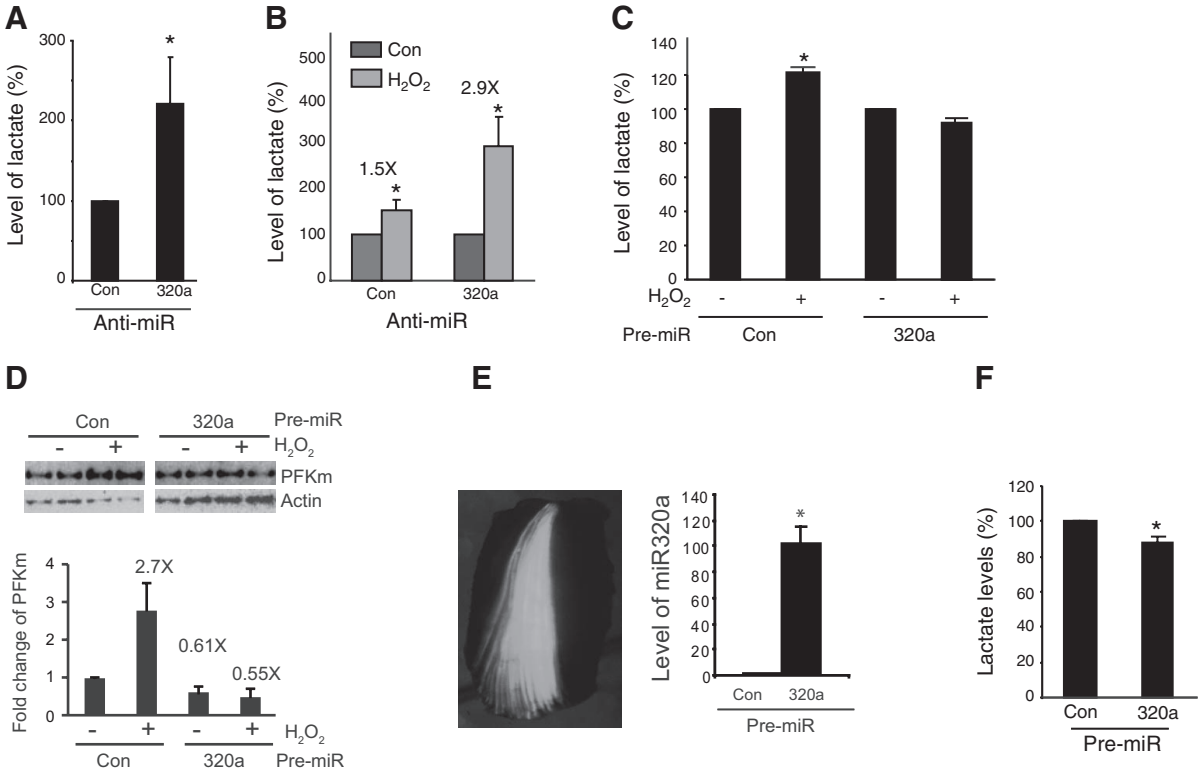

Figure 5. Mir-320a regulates glycolysis *in vitro* and *in vivo*. *A*) Reduction of miR-320a increases lactate level. Anti-miR-320a was transfected into C2C12 cells, and the intracellular level of lactate was measured ($n=3$). *B*) Lack of mir-320a sensitizes cells to oxidative stress-induced lactate production. Anti-miR-320a was transfected into C2C12 cells; 3 d later, the cells were treated with H_2O_2 40 μM for 24 h. Lactate level was measured. Note that anti-miR-320a-transfected cells accumulate more lactate in response to H_2O_2 treatment ($n=3$). *C, D*) Reduction in miR-320a is required for oxidative stress-induced glycolysis and the expression of PFKm. Transfected C2C12 cells (either control or pre-miR-320a, 40 nM) were treated with H_2O_2 (40 μm, 24 h). Lactate level was measured (*C*) and PFKm was detected by Western blot and quantitative data was acquired by normalizing to actin (*D*). *E–G*) MiR-320a regulates glycolysis *in vivo*. MiR-320a (320 nmol) was electroporated into TA muscle, together with GFP as reporter. *E*) Whole TA muscle under fluorescent microscope; white portion is the region of GFP^+ fibers. GFP^+ muscle fibers were isolated for both RNA and protein preparation. Quantitative PCR was used to detect the level of miR-320a in skeletal muscle (*E*), and equal amounts of total proteins were subjected to biochemical assay to detect the level of lactate (*F*) and Western blot analysis for detection of PFKm (*G*). Both actin and total protein (Ponceau S staining) are shown as controls. $^*P < 0.05$.

conditions it may help cells survive the stressful environment. If this hostile condition is sustained or overwhelming, however, the cells appear to lose this adaptive ability and move toward apoptotic pathways (21, 41).

Beyond the description of the glycolytic phenotype in these 2 biological systems, we have explored in this work the molecular mechanism underlying the development of this phenotype. We identify a novel posttranscriptional regulatory cascade *via* miR-320a that appears to be important to the activation of glycolysis in both VIDD and the Warburg Effect. MicroRNAs are short RNA molecules (19 to 25 nt), which bind to complementary sequences on target mRNA transcripts, *e.g.*, the 3′-UTR, usually resulting in translational repression and gene silencing, and they are known to play role in oxidative stress and cancer progression (42, 43). We show that miR-320a is significantly down-regulated in disused diaphragm, lung cancer, and cultured muscle cells subjected to H_2O_2-induced oxidative stress. We establish that down-regulated miR-320a results in increased levels of PFKm. PFKm is a crucial rate-limiting enzyme of glycolysis, without which glycolysis, as well as lactate production, are reduced (44). Although PFKm is a muscle-type PFK, surprisingly we find that it is also significantly induced in lung adenocarcinoma tissues. In addition to PFKm,

rom www.fasebj.org by Stanford University Libraries (171.65.8.159) on March 14, 2019. The FASEB Journal Vol. ${article.issue.getVolume()}, No. ${article.issue.getIssueNumber()},

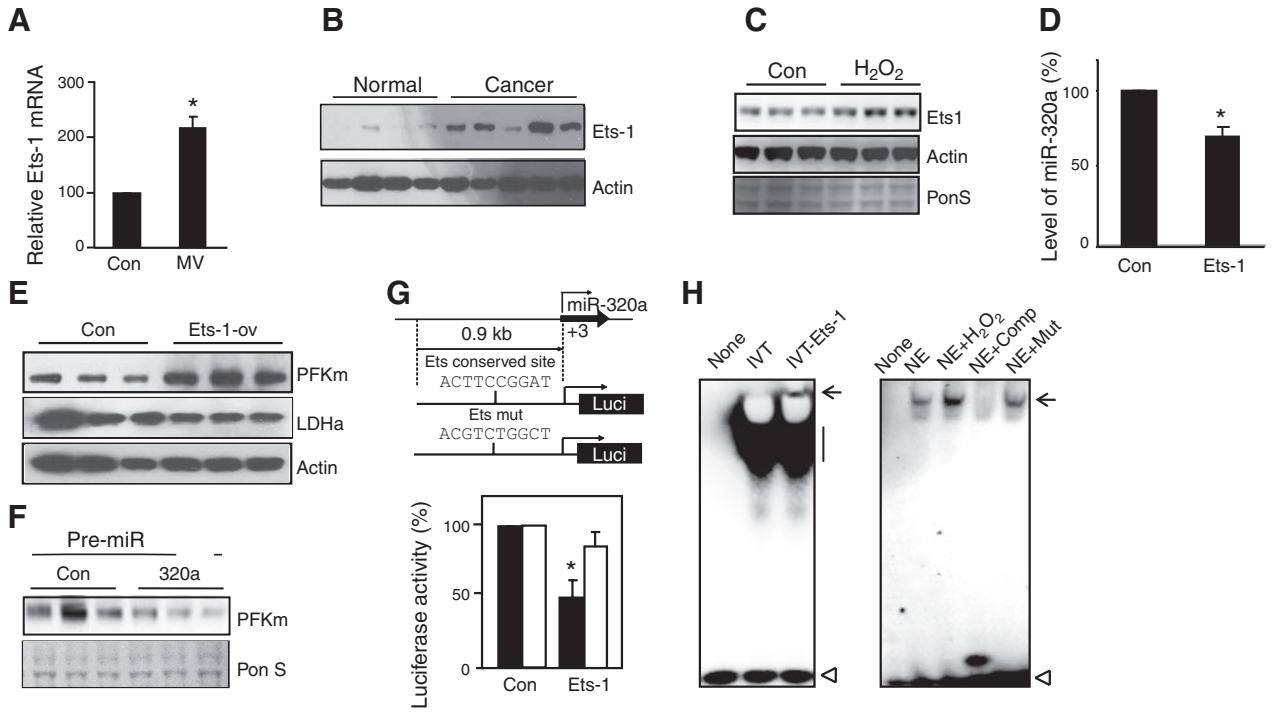

Figure 6. Ets-1 regulates the expression of miR-320a. *A–C*) Ets-1 expression is induced in MV human diaphragm muscle, lung adenocarcinoma, and H_2O_2-treated muscle cells. Real-time PCR was performed to measure the mRNA transcripts of Ets-1 in MV human diaphragm (*A*; $n=6$). Western blot analysis was performed to detect the protein levels of Ets-1 in lung adenocarcinoma (*B*), and H_2O_2-treated C2C12 muscle cells (*C*). Note: the Ets-1 protein level is undetectable in human diaphragm muscle. *D*, *E*) Ets-1 suppresses miR-320a and induces PFKm expression. Ets-1 expression vector was transfected into C2C12 cells and selected with G418 for 2 wk. Real-time PCR was performed to detect miR-320a expression in the C2C12 cells with constitutive Ets-1 expression (*D*; $n=3$). Western blot analysis was performed to detect the protein expression of PFKm from the cell lysate of Ets-overexpressing C2C12 cells (*E*; $n=3$). *F*) MiR-320a blocks the induction of PFKm in Ets-1-overexpressing cells. Pre-miR-320a was transfected into Ets-1-overexpressing C2C12 cells, and PFKm expression was detected by Western blot. *G*) Ets-1 regulates miR-320a promoter activity *via* Ets conserved site. The 5′-flanking DNA sequence of miR-320a and its Ets site mutated sequence were cloned into luciferase reporter constructs, and each was cotransfected with the Ets-1 expression vector. Luciferase assay was performed to detect the promoter activity normalized to the cotransfected CS2-β-Gal activity ($n=3$). *H*) Ets protein binds to the predicted Ets element in the miR-320a promoter sequence. *In vitro* translated (IVT) Ets-1 protein binds to the predicted Ets DNA element (left panel). Muscle extract binding to the predicted Ets DNA element was competed (100× access) by consensus sequence of Ets-1, but not by the Ets-site mutated sequence (right panel). None, probe only; NE, nuclear extract; Comp, consensus competition; Mut, Ets-mutated sequence competition. Arrow indicates DNA bound protein; straight line indicates nonspecific binding; open arrowhead indicates free DNA probe. $^*P < 0.05$.

miR-320a is also predicted to target other enzymes in the glycolytic pathway, such as pyruvate dehydrogenase kinase, isoform 3 (PDK3) and fructose-2,6-bisphosphotase (PFKFB2).

MiR-320a regulation of glycolysis may represent a general mechanism underlying other clinical diseases that are associated with changes in energy supply, including other cancers (45–47), cardiac and cerebral ischemia (48), and insulin resistance (49). With regard to malignancies, others have shown that miR-320a is down-regulated in colorectal (45), pancreatic (47), and breast cancer (46). It has also been reported that miR-320a targets transferrin receptor 1 and thus inhibits HL-60 cell proliferation (50). However, in none of this prior work has a link between miR-320a and glycolysis been made. Since the Warburg effect is thought to be important in many cancers, and since down-regulated miR-320a is associated with the induction of glycolysis in lung adenocarcinoma, we suggest that miR-320a may be directly related to the development of the malignant phenotype.

Ets-1 is a proto-oncogenic transcription factor that is known to be an important regulator of both cancer cell progression and metabolism (27). Ets-1 responds to oxidative stress by transcriptionally up-regulating many genes involved in energy metabolism (27, 51). In the current study, we find that Ets-1 protein is up-regulated in disused human diaphragm, lung cancer, and H_2O_2-treated muscle cells and that it suppresses the expression of miR-320a and increases PFKm protein expression. These findings are the first to link the function of Ets-1 protein to microRNAs, which may be a crucial step in rapidly and precisely controlling cellular energy metabolism in both cancer cells and disused diaphragm myofibers. Interestingly, miR-320a was recently reported to regulate Ets-2 (52), indicating that Ets family proteins may regulate each other *via* miR-320a.

Future work will involve blocking miR-320a in tumors and animal models of MV to determine whether this

rom www.fasebj.org by Stanford University Libraries (171.65.8.159) on March 14, 2019. The FASEB Journal Vol. ${article.issue.getVolume()}, No. ${article.issue.getIssueNumber()},

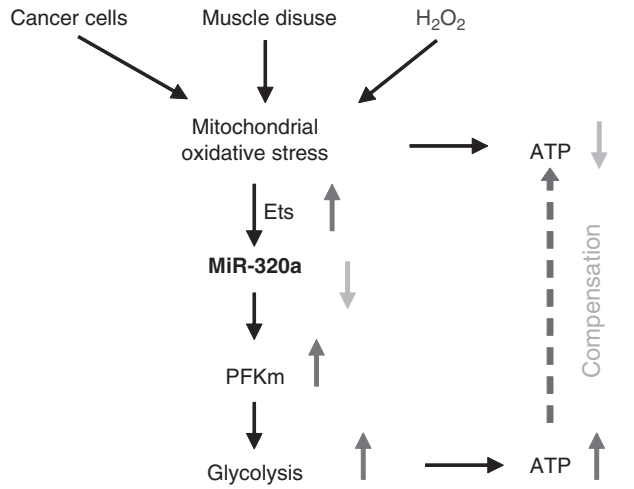

Figure 7. Schematic diagram of our proposed mechanism of the common regulation of glycolysis in lung adenocarcinoma and disused diaphragm muscle. Mitochondrial oxidative stress is a common to lung cancer, disused diaphragm muscle and H_2O_2-treated muscle cells. Ets-1 is induced by oxidative stress and suppresses miR-320a. Consequently, PFKm is induced, leading to partial compensation for the loss of ATP generation that results from mitochondrial dysfunction.

prevents up-regulation of glycolysis and the associated pathophysiology. One might also examine miR-320a in still other biological situations in which glycolysis is up-regulated to determine whether this is, in fact, a regulatory mechanism that controls glycolysis more broadly within nature.

This study advances the understanding of the pathophysiology of cancer and VIDD, and it suggests possible therapeutic avenues against disuse-associated muscle dysfunction and malignancy. In VIDD, a therapy that addresses both the atrophy and the dysfunction components of this process is likely to be most successful in avoiding ventilator-weaning problems and subsequent complications. Since oxidative stress appears to serve as a key event activating both the catabolic cascade and the shift to less efficient energy production, we believe that the use of mitochondria-targeted antioxidants to block both of these pathways may be valuable. This concept was tested in a recent publication (53) and indeed achieved promising results. In malignancy, blocking glycolysis could deprive cancers of a pathway that likely provides both an alternative energy supply and important building blocks for synthesis that allow cancer cell proliferation. FJ

The authors are grateful to Dr. Sabah Hussain (McGill University, Montreal, QC, Canada) for sharing MV limb muscle samples and Dr. Marlene Rabinovitch (Stanford University) for sharing the fluorescent dissection scope, Dr. Alejandro Sweet-Cordero (Stanford University) for helpful discussion and advice, and Dr. Xuhuai Ji (Stanford University) for assistance in microarray data analysis. This research was supported by a Veterans Affairs Merit Review grant awarded to J.B.S. and in part by U.S. National Institutes of Health grant RO1-HL-078834 to S.L. The authors disclosed the research results to Stanford Office of Licensing for potential intellectual property.

REFERENCES

1. Maughan, D. W., Henkin, J. A., and Vigoreaux, J. O. (2005) Concentrations of glycolytic enzymes and other cytosolic proteins in the diffusible fraction of a vertebrate muscle proteome. *Mol. Cell. Proteomics* **4,** 1541–1549
2. Crowther, G. J., Carey, M. F., Kemper, W. F., and Conley, K. E. (2002) Control of glycolysis in contracting skeletal muscle. I. Turning it on. *Am. J. Physiol. Endocrinol. Metab.* **282,** E67–73
3. Crowther, G. J., Kemper, W. F., Carey, M. F., and Conley, K. E. (2002) Control of glycolysis in contracting skeletal muscle. II. Turning it off. *Am. J. Physiol. Endocrinol. Metab.* **282,** E74–E79
4. Krause, U., and Wegener, G. (1996) Control of glycolysis in vertebrate skeletal muscle during exercise. *Am. J. Physiol.* **270,** R821–829
5. Ferreira, L. M. (2010) Cancer metabolism: the Warburg effect today. *Exp. Mol. Pathol.* **89,** 372–380
6. Xu, R. H., Pelicano, H., Zhou, Y., Carew, J. S., Feng, L., Bhalla, K. N., Keating, M. J., and Huang, P. (2005) Inhibition of glycolysis in cancer cells: a novel strategy to overcome drug resistance associated with mitochondrial respiratory defect and hypoxia. *Cancer Res.* **65,** 613–621
7. Brand, K. A., and Hermfisse, U. (1997) Aerobic glycolysis by proliferating cells: a protective strategy against reactive oxygen species. *FASEB J.* **11,** 388–395
8. Vander Heiden, M. G., Cantley, L. C., and Thompson, C. B. (2009) Understanding the Warburg effect: the metabolic requirements of cell proliferation. *Science* **324,** 1029–1033
9. Koppenol, W. H., Bounds, P. L., and Dang, C. V. (2011) Otto Warburg's contributions to current concepts of cancer metabolism. *Nat. Rev. Cancer* **11,** 325–337
10. Carew, J. S., and Huang, P. (2002) Mitochondrial defects in cancer. *Mol. Cancer* **1,** 9
11. Chandra, D., and Singh, K. K. (2011) Genetic insights into OXPHOS defect and its role in cancer. *Biochim. Biophys. Acta* **1807,** 620–625
12. Fogg, V. C., Lanning, N. J., and Mackeigan, J. P. (2011) Mitochondria in cancer: at the crossroads of life and death. *Chin. J. Cancer* **30,** 526–539
13. Gogvadze, V., Zhivotovsky, B., and Orrenius, S. (2010) The Warburg effect and mitochondrial stability in cancer cells. *Mol. Aspects. Med.* **31,** 60–74
14. Hockenbery, D. M. (2010) Targeting mitochondria for cancer therapy. *Environ. Mol. Mutagen.* **51,** 476–489
15. Jahnke, V. E., Sabido, O., Defour, A., Castells, J., Lefai, E., Roussel, D., and Freyssenet, D. (2010) Evidence for mitochondrial respiratory deficiency in rat rhabdomyosarcoma cells. *PLoS One* **5,** e8637
16. Najafov, A., and Alessi, D. R. (2010) Uncoupling the Warburg effect from cancer. *Proc. Natl. Acad. Sci. U. S. A.* **107,** 19135–19136
17. Sotgia, F., Martinez-Outschoorn, U. E., and Lisanti, M. P. (2011) Mitochondrial oxidative stress drives tumor progression and metastasis: should we use antioxidants as a key component of cancer treatment and prevention? *BMC Med.* **9,** 62
18. Ishii, N. (2007) Role of oxidative stress from mitochondria on aging and cancer. *Cornea* **26,** S3–9
19. Goh, J., Enns, L., Fatemie, S., Hopkins, H., Morton, J., Pettan-Brewer, C., and Ladiges, W. (2011) Mitochondrial targeted catalase suppresses invasive breast cancer in mice. *BMC Cancer* **11,** 191
20. Kavazis, A. N., Talbert, E. E., Smuder, A. J., Hudson, M. B., Nelson, W. B., and Powers, S. K. (2009) Mechanical ventilation induces diaphragmatic mitochondrial dysfunction and increased oxidant production. *Free Radic. Biol. Med.* **46,** 842–850
21. Tang, H., Lee, M., Budak, M. T., Pietras, N., Hittinger, S., Vu, M., Khuong, A., Hoang, C. D., Hussain, S. N., Levine, S., and Shrager, J. B. (2011) Intrinsic apoptosis in mechanically ventilated human diaphragm: linkage to a novel Fos/FoxO1/Stat3-Bim axis. *FASEB J.* **25,** 2921–2936
22. Hussain, S. N., Mofarrahi, M., Sigala, I., Kim, H. C., Vassilakopoulos, T., Maltais, F., Bellenis, I., Chaturvedi, R., Gottfried, S. B., Metrakos, P., Danialou, G., Matecki, S., Jaber, S., Petrof, B. J., and Goldberg, P. (2010) Mechanical ventilation-induced diaphragm disuse in humans triggers autophagy. *Am. J. Respir. Crit. Care Med.* **182,** 1377–1386

rom www.fasebj.org by Stanford University Libraries (171.65.8.159) on March 14, 2019. The FASEB Journal Vol. ${article.issue.getVolume()}, No. ${article.issue.getIssueNumber()},

23. Tang, H., and Goldman, D. (2006) Activity-dependent gene regulation in skeletal muscle is mediated by a histone deacetylase (HDAC)-Dach2-myogenin signal transduction cascade. *Proc. Natl. Acad. Sci. U. S. A.* **103,** 16977–16982
24. Nye, J. A., Petersen, J. M., Gunther, C. V., Jonsen, M. D., and Graves, B. J. (1992) Interaction of murine ets-1 with GGA-binding sites establishes the ETS domain as a new DNA-binding motif. *Genes Dev.* **6,** 975–990
25. Rády, P., Arany, I., Boján, F., and Kertai, P. (1979) Activities of four glycolytic enzymes (HK, PFK, PK, and LDH) and isozymic pattern of LDH in mouse lung tumor induced by urethan. *J. Cancer Res. Clin. Oncol.* **95,** 287–289
26. Chen, G., Gharib, T. G., Wang, H., Huang, C. C., Kuick, R., Thomas, D. G., Shedden, K. A., Misek, D. E., Taylor, J. M., Giordano, T. J., Kardia, S. L., Iannettoni, M. D., Yee, J., Hogg, P. J., Orringer, M. B., Hanash, S. M., and Beer, D. G. (2003) Protein profiles associated with survival in lung adenocarcinoma. *Proc. Natl. Acad. Sci. U. S. A.* **100,** 13537–13542
27. Verschoor, M. L., Wilson, L. A., Verschoor, C. P., and Singh, G. (2010) Ets-1 regulates energy metabolism in cancer cells. *PLoS One* **5,** e13565
28. Levine, S., Nguyen, T., Taylor, N., Friscia, M., Budak, M., Rothenberg, P., Zhu, J., Sachdeva, R., Sonnad, S., Kaiser, L., Rubinstein, N., Powers, S., and Shrager, J. (2008) Rapid disuse atrophy of diaphragm fibers in mechanically ventilated humans. *N. Engl. J. Med.* **358,** 1327–1335
29. Jaber, S., Petrof, B. J., Jung, B., Chanques, G., Berthet, J. P., Rabuel, C., Bouyabrine, H., Courouble, P., Koechlin, C., Sebbane, M., Similowski, T., Scheuermann, V., Mebazaa, A., Capdevila, X., Mornet, D., Mercier, J., Lacampagne, A., Philips, A., and Matecki, S. (2011) Rapidly progressive diaphragmatic weakness and injury during mechanical ventilation in humans. *Am. J. Respir. Crit. Care Med.* **183,** 364–371
30. Shanely, R., Van Gammeren, D., Deruisseau, K., Zergeroglu, A., McKenzie, M., Yarasheski, K., and Powers, S. (2004) Mechanical ventilation depresses protein synthesis in the rat diaphragm. *Am. J. Respir. Crit. Care. Med.* **170,** 994–999
31. Fredriksson, K., Radell, P., Eriksson, L. I., Hultenby, K., and Rooyackers, O. (2005) Effect of prolonged mechanical ventilation on diaphragm muscle mitochondria in piglets. *Acta Anaesthesiol. Scand.* **49,** 1101–1107
32. Allen, D. G., Lamb, G. D., and Westerblad, H. (2008) Skeletal muscle fatigue: cellular mechanisms. *Physiol. Rev.* **88,** 287–332
33. Leite, T. C., Coelho, R. G., Da Silva, D., Coelho, W. S., Marinho-Carvalho, M. M., and Sola-Penna, M. (2011) Lactate down-regulates the glycolytic enzymes hexokinase and phosphofructokinase in diverse tissues from mice. *FEBS Lett.* **585,** 92–98
34. Liu, C., Wu, J., Zhu, J., Kuei, C., Yu, J., Shelton, J., Sutton, S. W., Li, X., Yun, S. J., Mirzadegan, T., Mazur, C., Kamme, F., and Lovenberg, T. W. (2009) Lactate inhibits lipolysis in fat cells through activation of an orphan G-protein-coupled receptor, GPR81. *J. Biol. Chem.* **284,** 2811–2822
35. Gatenby, R. A., and Gillies, R. J. (2004) Why do cancers have high aerobic glycolysis? *Nat. Rev. Cancer* **4,** 891–899
36. Kauhanen, S., von Boguslawsky, K., Michelsson, J. E., and Leivo, I. (1998) Satellite cell proliferation in rabbit hindlimb muscle following immobilization and remobilization: an immunohistochemical study using MIB 1 antibody. *Acta Neuropathol.* **95,** 165–170
37. Wu, S. B., and Wei, Y. H. (2012) AMPK-mediated increase of glycolysis as an adaptive response to oxidative stress in human cells: implication of the cell survival in mitochondrial diseases. *Biochim. Biophys. Acta* **1822,** 233–247
38. Danshina, P. V., Schmalhausen, E. V., Avetisyan, A. V., and Muronetz, V. I. (2001) Mildly oxidized glyceraldehyde-3-phosphate dehydrogenase as a possible regulator of glycolysis. *IUBMB Life* **51,** 309–314
39. Liddell, J. R., Zwingmann, C., Schmidt, M. M., Thiessen, A., Leibfritz, D., Robinson, S. R., and Dringen, R. (2009) Sustained hydrogen peroxide stress decreases lactate production by cultured astrocytes. *J. Neurosci. Res.* **87,** 2696–2708
40. Colussi, C., Albertini, M. C., Coppola, S., Rovidati, S., Galli, F., and Ghibelli, L. (2000) H2O2-induced block of glycolysis as an active ADP-ribosylation reaction protecting cells from apoptosis. *FASEB J.* **14,** 2266–2276
41. Siu, P. M., Wang, Y., and Alway, S. E. (2009) Apoptotic signaling induced by H2O2-mediated oxidative stress in differentiated C2C12 myotubes. *Life Sci.* **84,** 468–481
42. Hulsmans, M., De Keyzer, D., and Holvoet, P. (2011) MicroRNAs regulating oxidative stress and inflammation in relation to obesity and atherosclerosis. *FASEB J.* **25,** 2515–2527
43. Calin, G. A., and Croce, C. M. (2006) MicroRNA signatures in human cancers. *Nat. Rev. Cancer* **6,** 857–866
44. García, M., Pujol, A., Ruzo, A., Riu, E., Ruberte, J., Arbós, A., Serafín, A., Albella, B., Felíu, J. E., and Bosch, F. (2009) Phosphofructo-1-kinase deficiency leads to a severe cardiac and hematological disorder in addition to skeletal muscle glycogenosis. *PLoS Genet.* **5,** e1000615
45. Schepeler, T., Reinert, J. T., Ostenfeld, M. S., Christensen, L. L., Silahtaroglu, A. N., Dyrskjøt, L., Wiuf, C., Sørensen, F. J., Kruhøffer, M., Laurberg, S., Kauppinen, S., Ørntoft, T. F., and Andersen, C. L. (2008) Diagnostic and prognostic microRNAs in stage II colon cancer. *Cancer Res.* **68,** 6416–6424
46. Yan, L. X., Huang, X. F., Shao, Q., Huang, M. Y., Deng, L., Wu, Q. L., Zeng, Y. X., and Shao, J. Y. (2008) MicroRNA miR-21 overexpression in human breast cancer is associated with advanced clinical stage, lymph node metastasis and patient poor prognosis. *RNA* **14,** 2348–2360
47. Lee, K. H., Lotterman, C., Karikari, C., Omura, N., Feldmann, G., Habbe, N., Goggins, M. G., Mendell, J. T., and Maitra, A. (2009) Epigenetic silencing of MicroRNA miR-107 regulates cyclin-dependent kinase 6 expression in pancreatic cancer. *Pancreatology* **9,** 293–301
48. Sepramaniam, S., Armugam, A., Lim, K. Y., Karolina, D. S., Swaminathan, P., Tan, J. R., and Jeyaseelan, K. (2010) MicroRNA 320a functions as a novel endogenous modulator of aquaporins 1 and 4 as well as a potential therapeutic target in cerebral ischemia. *J. Biol. Chem.* **285,** 29223–29230
49. Ling, H. Y., Ou, H. S., Feng, S. D., Zhang, X. Y., Tuo, Q. H., Chen, L. X., Zhu, B. Y., Gao, Z. P., Tang, C. K., Yin, W. D., Zhang, L., and Liao, D. F. (2009) Changes in microRNA profile and effects of miR-320 in insulin-resistant 3T3-L1 adipocytes. *Clin. Exp. Pharmacol. Physiol.* **36,** e32–e39
50. Schaar, D. G., Medina, D. J., Moore, D. F., Strair, R. K., and Ting, Y. (2009) miR-320 targets transferrin receptor 1 (CD71) and inhibits cell proliferation. *Exp. Hematol.* **37,** 245–255
51. Wilson, L. A., Gemin, A., Espiritu, R., and Singh, G. (2005) ets-1 is transcriptionally up-regulated by H2O2 *via* an antioxidant response element. *FASEB J.* **19,** 2085–2087
52. Bronisz, A., Godlewski, J., Wallace, J. A., Merchant, A. S., Nowicki, M. O., Mathsyaraja, H., Srinivasan, R., Trimboli, A. J., Martin, C. K., Li, F., Yu, L., Fernandez, S. A., Pécot, T., Rosol, T. J., Cory, S., Hallett, M., Park, M., Piper, M. G., Marsh, C. B., Yee, L. D., Jimenez, R. E., Nuovo, G., Lawler, S. E., Chiocca, E. A., Leone, G., and Ostrowski, M. C. (2012) Reprogramming of the tumour microenvironment by stromal PTEN-regulated miR-320. *Nat. Cell Biol.* **14,** 159–167
53. Powers, S. K., Hudson, M. B., Nelson, W. B., Talbert, E. E., Min, K., Szeto, H. H., Kavazis, A. N., and Smuder, A. J. (2011) Mitochondria-targeted antioxidants protect against mechanical ventilation-induced diaphragm weakness. *Crit. Care. Med.* **39,** 1749–1759

Received for publication March 14, 2012.
Accepted for publication June 20, 2012.

rom www.fasebj.org by Stanford University Libraries (171.65.8.159) on March 14, 2019. The FASEB Journal Vol. ${article.issue.getVolume()}, No. ${article.issue.getIssueNumber()},